

# Rear Wing Aerodynamic Influence on F1 Car Cornering Ability

**Dhairya Parikh**

Cathedral and John Connon School dhairyaparikh.92@gmail.com

**Reetu Jain**

Mentor, On My Own Technology Pvt Ltd reetu.jain@onmyowntechnology.com

**Abstract**—Lap timings are affected by a variety of elements in the motorsport business. These cars' aerodynamics are critical on both straight and curving tracks. This study investigates the aerodynamic impact of different rear wing layouts on the maneuverability of a Formula 1 (F1) car. The study looked at three wing configurations: a single wing at an angle of attack of 18 degrees, a double wing at an angle of attack of 18 degrees with the Drag Reduction System (DRS) turned off, and a double wing at an angle of attack of 0 degrees with the DRS turned on. The total downward force produced by each set of wings at an 18-degree banking angle, the normal acceleration in  $m/s^2$ , and the turning radius in meters are all taken into account in the calculations.

**Keywords**—Five keywords.

## I. INTRODUCTION

F1 racing is well-known for its high-speed daring maneuvers and precision driving, in which drivers push themselves and their vehicles to their utmost. F1 cars' aerodynamic design is important to their track performance. The purpose of this study is to look at the effect of an F1 car's rear wing on its cornering radius. Rear wings contribute significantly to downforce generation, which is critical for maintaining traction and stability during high-speed cornering. The complicated relationship between rear-wing aerodynamics and the consequent cornering radius is presently being studied. Understanding the effect of the rear wing on the cornering radius allows teams to improve and optimize their F1 car design and setup to get the best performance. Not only will this knowledge aid racing teams, but it will also benefit the automotive industry, leading to breakthroughs in road car handling and safety systems.

The primary objectives of this research are to investigate the relationship between rear wing design parameters (such as angle of attack, height, and width) and the resulting cornering radius of an F1 car, and to make recommendations for optimizing rear wing design and setup to achieve desired cornering performance in F1 cars. In this study, Modern computational fluid dynamics (CFD) simulations were integrated with real-world track data and vehicle

aerodynamic models to provide a thorough grasp of this complicated interplay. The combination of these various disciplines seeks to provide practical assistance for optimizing rear wing design and setup, pushing the limits of F1 performance.

## II. LITERATURE REVIEW

D Martins et al. [1] investigated the aerodynamic interaction of a three-element wing with the wheel-ground effect, with a focus on revisions to the front wing layout mandated by Formula One regulations in 2022. Using a simplified model of a Formula One car and a computational fluid dynamics analysis, the effect of altering the incidence of the second flap on the front wing on the wheel wake was explored. The results showed that changing the flap configurations altered the upwash flow fields, causing changes in the separation point on top of the tire and altering wheel wake properties including length and direction.

M Basso et al. [2] studied the aerodynamic performance and interactions of a Gurney Flap (GF) fitted on the front wing of a racing car. To understand the flow structure and performance of the components, a full CFD simulation of an F1 car configuration was performed. The GF had a significant impact on the overall flow structure, increasing front wing downforce by 24% and drag force by 28%. The GF amplified the ground effect, causing the flow to interact with other components such as the endplate and wheel group. Correct dimensioning may result in greater aerodynamic downforce and efficiency than the baseline.

Seljak et al [3] concentrated on minimizing air drag to attain high speeds, but they encountered stability concerns due to lift forces at high velocities. The use of inverted wing profiles to generate negative lift was established in the late 1920s, although Formula One did not explore the potential of downforce until the late 1960s. The front wing, which accounts for around one-third of the car's downforce, was modified more than the rear wing. It began with a simple rectangular airfoil with vertical endplates and was later improved with the Gurney flap in 1971 and the introduction of multi-element wings in 1984. To improve flow conditions and counterbalance rules, innovations such as elevating the car's nose and curving the front wing were introduced.

This report delves into the evolution of Toet et al.

[4]'s research methodology in aerodynamics inside the Formula 1 (F1) sector. It covers how F1 teams initially focused on improving the realism of aero testing, later adding mathematical simulations with physical testing. The change from studying only global forces to regulating flow structures around the car highlights the complexity of the flow field and the numerous methods used by different teams. Despite the restrictions of sharing proprietary material, this report provides useful insights into historical advancements and contemporary issues in F1 aerodynamics.

This paper discusses the importance of aerodynamic downforce in improving racing vehicle performance. McKay et al. [5] investigate the limits imposed by racing rules and practical concerns on the generation of downforce, such as wing size, shape, and the location of the aerodynamic center of pressure (CP). The trade-off between greater downforce and higher aerodynamic drag is investigated. The effects of wing downforce on racecar performance are examined using steady-state cornering, straight-line braking, and acceleration. The effect of wing aerodynamics on racecar performance characteristics is presented, and the preference for higher-lift airfoils for turning and braking conditions, albeit with reduced acceleration performance, is highlighted.

The advances in methodologies and understanding brought about by X Zhang et al. [6]'s concentration on aerodynamics have contributed to the increased speeds attained by Formula 1 cars. The authors discuss the advancements made in ground effect aerodynamics of open-wheel race cars in this work, with a focus on fundamental aerodynamics rather than practical applications. The important phenomena and force regimes connected with ground effect aerodynamics are discussed, as are the key aerodynamic components such as wings, diffusers, and wheels. The relationship between ride height and downforce is presented, demonstrating that lowering the ride height initially increases downforce until a maximum value is reached. Downforce is reduced and eventually disappears as the ride height is reduced more.

A J Marn et al. [7] use numerical approaches to come out on top in car contests by optimizing the design of a rear wing. Full-scale 3D numerical modelling and the application of the SST turbulent flow model, spinning wheels, and a moving road allow for successful simulations of multi-section wings. The main issue is flow separation, which can be avoided by using a slat before the main wing instead of a second flap. Furthermore, the use of 3D wing variants and well-designed end plates is emphasized, as they contribute to the development of side vortices and the prevention of downstream flow disturbances. Higher angles of attack and elevated main wing locations are proven to improve downforce by minimizing flow separation.

According to Modi et al. [8], in the early days of

Formula One racing, unequal races, and dangerous scenarios emerged due to the lack of power and size limits. The FIA created rules to solve these difficulties, establishing fairness, and safety, and promoting clean racing. Inverted wings were introduced in Formula One in 1968, and they revolutionized the sport by producing tremendous downforce and enhanced aerodynamic performance. The suggested split rear wing layout gives you more control by allowing you to vary the angle of attack as well as the Anhedral/Dihedral angle.

Gyawali et al. [9] show the numerous features of a single-seat, open-cockpit, open-wheel aircraft with visible front and rear wings and an engine positioned behind the driver. According to the study's modelling results, increasing the camber line of the car's airfoil may result in additional downforce, as shown by a negative lift coefficient. This is achieved by increasing airflow at the bottom of the airfoil, which results in decreased pressure. Furthermore, it was determined that angling the Drag Reduction System (DRS) wing during turning boosts tire traction while keeping it horizontal decreases drag and allows for faster straightaways.

Buljac et al. [10] used aerodynamic improvements to improve road vehicle fuel efficiency, traction, and stability. Increase the tire's normal force to increase the maximum lateral force, which improves traction and cornering. This is accomplished by the use of aerodynamic devices that provide downforce while neutralizing uplift force, hence enhancing vehicle dynamics without increasing mass. The rear wing, which looks like an airfoil and is located in the trunk of the car, is frequently used to improve aerodynamics. The objective is to maximize downforce, traction, and stability while minimizing drag and fuel consumption. The rear wing enhances vertical stability while minimizing the frequency of rear vortices in the vehicle wake, according to research. The ideal rear wing locations have been determined, and a maximum downforce-to-drag ratio of 0.57 is achieved at 39% of the height between the top trunk surface and the roof.

In this study, JCM et al. [11] studied the performance effects of adding front and rear wings to a Formula SAE automobile. A mathematical transient model was used, which was based on 2D Computational Fluid Dynamics (CFD) data and analytical equations. Through lap time analysis, ideal values for downforce and drag coefficient were discovered by evaluating different combinations of airfoil and wing geometry. The results showed that the aerodynamic package greatly enhanced the car's performance in the main dynamic events of the Formula SAE championship. The significance of a negative lift coefficient for cornering events was emphasized, resulting in faster cornering speeds and shorter braking distances. Drag forces were not a constraint in the endurance event, allowing for larger improvements in the negative lift.

The goal of this effort is to passively reduce the

induced drag of a Formula One car's rear wing at high speeds via aeroelastic tailoring. Thuwis et al. [12] found that increasing the angle of attack of the rear wing increases downforce and produces drag at higher speeds. A composite torsion box design is used, with upper and lower skins that are extension-shear connected, allowing for bending-torsion coupling. A three-dimensional static aeroelastic study is performed to optimize the wing for the least induced drag while preserving the necessary downforce during low-speed turns using a response surface methodology.

The study conducted by J Katz et al. [13] looked at the effects of different geometrical modifications on the rear-wing form of a race car on its high-lift aerodynamic characteristics. Numerous wing shapes can be explored without the requirement for time-consuming and expensive wind tunnel models due to numerical simulation techniques. The outcomes showed that a rear wing that complied with CART requirements could obtain a lift coefficient of roughly -2.2 depending on the wing's reference area. Additionally, it was discovered that the amount of downforce produced by the car was boosted by the aerodynamic contact between the rear wing and the body of the car, particularly the underbody channels.

In this study, F Fauzun et al. [14] demonstrates the critical significance of aerodynamics in reaching ideal race times by utilizing the wind's force to increase speed. Various studies have examined aerodynamic improvements using methods such as CFD analysis, experimental testing, and undertray changes. Reduced drag coefficients and enhanced performance in dynamic events among the results of these experiments. For instance, adding wings to Formula Student cars has sped up skidpad speeds, while undertray changes and outlet angle tweaks have enhanced downforce and decreased drag forces. The addition of a DRS (Drag Reduction System) system significantly decreased drag further.

Dominy et al. [15] have examined the hitherto unheard-of levels of aerodynamic improvement in Grand Prix vehicles and the significant financial investments made by teams in wind tunnels, machinery, models, and personnel. High cornering speeds and significant performance improvements have resulted from the potential benefits of improved aerodynamic designs, particularly in the generation of downforce. The lap time can be shaved off by 0.1 seconds with just a 1% increase in downforce. The outward similarities of F1 cars have, however, converged due to stable racing regulations, and the differences in performance can be noticed in the precise variables of their aerodynamic design.

The goal of this study was to understand how the rear wing affected the cornering radius of an F1 car. By examining this relationship, it was anticipated to improve auto safety regulations, enhance vehicle handling, and progress motorsports technology. Insightful information was offered for racing teams, engineers, and enthusiasts alike through a novel

approach and in-depth research, resulting in more exciting competition and faster lap times.

### III. METHODOLOGY

Fusion 360 was used to build three different sorts of 3D models for this investigation. These variants have a single rear wing, a double rear wing with an angle of attack of 18 degrees when DRS is off, and a third double rear wing with an angle of attack of zero degrees when DRS is on. The vertical distance between the two wings on these models is 35mm. The width is 100mm, and the wing cord size is 100mm. Three figures, 1, 2, and 3 below, show the different wings that were used to carry out the CFD analysis.

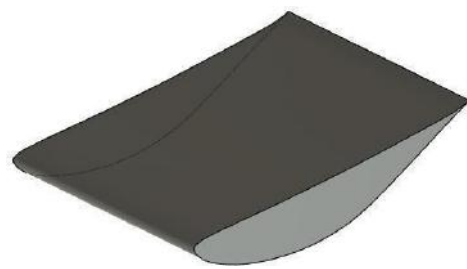


Fig 1. Single Rear Wing

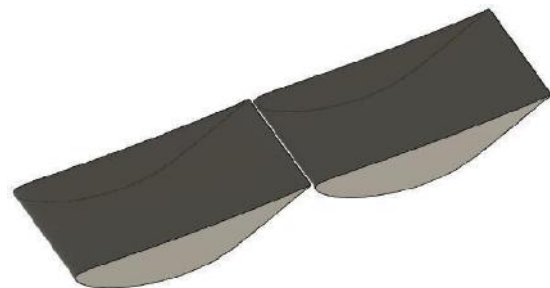


Fig 2. Double Rear wing DRS OFF Condition



Fig 3. Double wing DRS ON Condition

The simulation setup involved creating a wind tunnel, mesh generation with the relevant properties,

and naming conventions after the 3D model was ready. The drag and lift forces were then calculated using the solver's specified settings.

The 3D model was first imported into ANSYS Fluent's design module, where a wind tunnel was built around it to replicate accurate fluid flow conditions. To simulate a wind tunnel test, a Boolean operation was used to create a fluid volume inside the wind tunnel. The design module made additional alterations to the model, concentrating on the size and shape of the rear wing in particular.

The redesigned model was then loaded into ANSYS Fluent's Mesh module. To optimally utilize processing power, a finer mesh was chosen close to the wing and a coarser mesh in other parts of the fluid zone. To ensure the integrity of the mesh, special consideration was paid to maintaining the ideal orthogonal quality and aspect ratio. Additionally, a naming scheme was developed for the mesh's various portions to make the analysis simpler. These mesh parts were given specific names, such as velocity intake, pressure outlet, wall, ground, top, and wing-body, which were helpful in the ensuing solver setup step. The mesh model was then imported into ANSYS Fluent's setup module with the appropriate name selection, and the following setup was carried out: Due to the incompressibility of the flow and the absolute nature of the velocity formulation, the solver was programmed to use a pressure-based approach. The boundary layer around the wing was accurately captured by the K- epsilon (2 equ.)-Realizable model with a non-equilibrium wall function, improving the quality of the results. The inlet velocity at the velocity inlet was set at 104 m/s with the substance being air. For the purposes of the solution techniques, the gradient was made to be least square cell- based, and the pressure, momentum, and turbulent kinetic energy were calculated using a second-order upwind scheme. A monitor was added to record the drag and lift. The calculation was then executed until convergence was achieved.

The Drag and lift forces have been noted down which is further discussed in the result section of the Research paper.

#### IV. RESULT AND DISCUSSIONS

**TABLE I:** Values of Drag and Lift Forces from the CFD simulation for various Wing setups.

Type of Wing Setups	Drag Force in N	Lift Force in N
Single wing at an 18degree angle of attack	28.017928	-102.13772
Double wing at an 18degree angle of attack DRS OFF	91.662122	-324.63749
Double wing at 0-degree angle of attack DRS ON	14.235435	-223.6396

Table 1 above displays the findings from the CFD analysis of various wing arrangements. Each wing configuration's drag and lift values were listed together with the accompanying negative lift forces,

which signify downward pulls on the wings. Further calculations were made based on these findings to ascertain the total downward force, standard acceleration, and cornering radius at an 18- degree banking angle. Each wing setup underwent the calculations, which are displayed in Table 1.

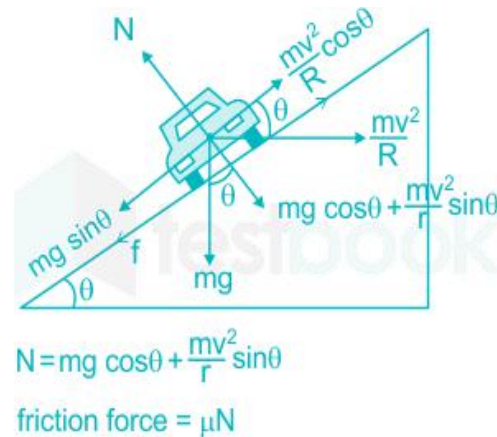


Fig 4. The CFD analysis  
Explanation of the image:

Where,

$$\begin{aligned}
 & m = \text{Mass of vehicle in kg} \\
 & \text{Consider value, } 960\text{kg (Mass of vehicle + Mass of driver)} \\
 & v = \text{Velocity of vehicle in } \text{ms}^{-1} \\
 & r = \text{Radius of curvature in m} \\
 & \theta = \text{Angle of banking in degree } (^{\circ}) \\
 & f = \text{Frictional force in N} \\
 & N = \text{Normal reaction in N} \\
 & g = \text{Gravitational constant in } \text{ms}^{-2} \\
 & \mu = \text{Coefficient of friction} \\
 & \text{Total Downward force } (F_D) \text{ at an angle of banking of } 18^{\circ} = mg \cos(\theta) + \text{Downward force value from CFD simulation } (F_{D,CFD}) \\
 & \text{Normal acceleration } (a_N) = \frac{\text{Total Downward force } (F_D) \text{ at an angle of banking of } 18^{\circ}}{\text{Mass of vehicle (m)}} \\
 & \text{Cornering Radius in m } (\rho) = \frac{v^2}{a_N}
 \end{aligned}$$

The first equation deals with the vehicle's total downward force  $FD$  as it goes along the banked curve. This power is made up of two parts. The first component,  $mg \cos \theta$ , accounts for the gravitational force that pulls the vehicle downward. The cosine of the banking angle  $\theta$  is used to compute the percentage of gravity acting perpendicular to the road surface. The second component is, reflects the additional downward force calculated from computational fluid dynamics simulations that take aerodynamics and air resistance into account.

In the second equation, normal acceleration  $a_N$  is the rate of change of the vehicle's speed perpendicular to the road surface. It is influenced by the vehicle's total downward force  $FD$ . The equation divides this force by the vehicle's mass ( $m$ ) to calculate how quickly the vehicle's speed changes as it follows the curved course.

Finally, the cornering radius equation links the velocity  $v$  and normal acceleration  $a_N$  of the vehicle to the curvature of the road. A centripetal force directed towards the center of the curve is required to keep a vehicle on track as it travels around a curve.

This centripetal force is provided by normal acceleration, and the cornering radius formula demonstrates that the radius of the curve (how sharp the curve is) is inversely proportional to the square of the vehicle's speed and directly related to normal acceleration.

*A. Calculations of Cornering radius at maximum speed and an angle of banking 18 degrees*

**TABLE II:** Calculations of Cornering radius at maximum speed and an angle of banking 18 degrees

Type of wing setup	Total downward force at an angle of banking 18-degree	Normal acceleration in m/s <sup>2</sup>	cornering radius in m
Single wing at an 18degree angle of attack	9227.27N	9.612	1125.26
Double wings at an 18degree angle of attack DRS OFF	9438.89	9.832	1100
Double wing at 0-degree angle of attack DRS ON	9151.66	9.532	1134.7

By examining the data, it is clear that the single wing, which was attacking at an angle of 18 degrees, produced a total downward force of 9227.27 N, a normal acceleration of 9.612 m/s<sup>2</sup>, and a turning radius of 1125.26 m. The total downward force increased to 9438.89 N for the double wing at an 18-degree angle of attack with DRS OFF, resulting in a higher normal acceleration of 9.832 m/s<sup>2</sup> and a smaller cornering radius of 1100 m. In contrast, the double wing produced a total downward force of 9151.66 N at a 0-degree angle of attack with DRS ON. This setup displayed a typical acceleration of 9.532 m/s<sup>2</sup> and a cornering radius of 1134.7 m.

*B. Calculation of maximum cornering speed when an angle of banking was 18 degrees and Cornering radius 800m.*

**TABLE III:** Calculation of maximum cornering

Type of wing setup	If the angle of banking is 18 degrees and the corner radius is 800m then the speed at which a car can take a turn in Km/Hr
Single wing at an 18degree angle of attack	315.68
Double wings at an 18degree angle of attack DRS OFF	319.25
Double wing at 0-degree angle of attack DRS ON	314.352

speed when an angle of banking was 18 degrees and Cornering radius 800m. Based on Table 3, which presents the speed at which the car can take a turn for different wing setups, the angle of banking at 18 degrees, and a corner radius of 800 meters, the following observations can be made:

The car can turn at a speed of 315.68 km/h for the single wing at an 18-degree angle of attack. This shows that the automobile can maintain stability and maneuverability with this wing layout while negotiating an 800-meter-radius turn at quite high speeds. The car can also make the bend at a slightly faster speed of 319.25 km/h because of the double

wing at an 18-degree angle of attack with DRS OFF. The car can handle the turn with greater control and efficiency because of the additional downforce produced by the double wing arrangement, which also helps to maintain traction and stability. The speed at which the vehicle can make the turn, estimated at 314.352 km/h, is somewhat lower for the double wing at a 0-degree angle of attack with DRS ON. Even while this setup produces less downforce than the DRS OFF level, it still offers enough stability and control to successfully navigate the turn.

**CONCLUSION**

The results have been observed to follow aerodynamic principles. Compared to single-wing configurations, double-wing arrangements generate more downforce, improving stability and cornering performance. Overall, the findings reveal that the wing configuration chosen has a considerable impact on the speed at which an F1 car can safely negotiate a curve with a specific banking degree and corner radius. Higher speeds are attainable with double-wing configurations, whether DRS is turned on or off. The highest overall downward force is believed to be produced by deploying a double wing at an 18-degree angle of attack and turning off DRS, resulting in greater cornering capabilities with a reduced cornering radius.

The findings help to clarify how various wing layouts affect an F1 car's overall performance and handling qualities. Decisions about aerodynamic design and setup adjustments can be made with the help of useful insights that can improve cornering performance and improve lap times on race circuits. For race teams and engineers working to optimize the aerodynamics of F1 cars for particular track conditions and cornering needs, these insights are important. Teams may establish the appropriate speed at which the car can safely navigate bends without compromising stability and control by taking into account the banking angle, corner radius, and wing setup.

**REFERENCES**

- [1] Martins, Daniel, João Correia, and André Silva. "The influence of front wing pressure distribution on wheel wake aerodynamics of an F1 car." *Energies* 14.15 (2021): 4421.
- [2] Basso, Mattia, Carlo Cravero, and Davide Marsano. "Aerodynamic effect of the gurney flap on the front wing of an F1 car and flow interactions with car components." *Energies* 14.8 (2021): 2059.
- [3] Seljak, Gregor. "Race car aerodynamics." University of Ljubljana Faculty of mathematics and physics, Department of physics (2008).
- [4] Toet, Willem. "Aerodynamics and aerodynamic research in Formula 1." *The Aeronautical Journal* 117.1187 (2013): 1-26.
- [5] McKay, Noah J., and Ashok Gopalathnam. "The effects of wing aerodynamics on race vehicle performance." *SAE Transactions* (2002):

2254-2263.

- [6] Zhang, Xin, Willem Toet, and Jonathan Zerihan. "Ground effect aerodynamics of race cars." (2006): 33-49.
- [7] Iljaž, Jurij, et al. "Optimization of SAE formula rear wing." *Strojniški vestnik-Journal of Mechanical Engineering* 62.5 (2016): 263-272.
- [8] Modi, Aryaman, and Rejin Jacob. "Analysis of a Split Dihedral and Anhedral Arrangement of the Rear Wing of a Formula One Car." (2022).
- [9] Gyawali, Lekhnath. "CFD ANALYSIS OF DUAL ELEMENT REAR WING OF A F1 CAR."
- [10] Buljac, A., et al. "Automobile aerodynamics influenced by airfoil- shaped rear wing." *International journal of automotive technology* 17 (2016): 377-385.
- [11] Rodrigues, Julio Cesar Martinelli, and Rodrigo de Souza Vieira. Evaluation of the effects of adding front and rear wings on the lap times of a Formula SAE car. No. 2012-36-0136. SAE Technical Paper, 2012.
- [12] Thus, Glenn AA, et al. "Aeroelastic tailoring using lamination parameters: Drag reduction of a Formula One rear wing." *Structural and Multidisciplinary Optimization* 41 (2010): 637-646.
- [13] Katz, Joseph, and Lee Dykstra. Study of an open-wheel racing car's rear-wing aerodynamics. No. 890600. SAE Technical Paper, 1989.
- [14] Fauzun, Fauzun, and Gilang Sandy Firdaus. "Effect of undertray inlet angle and drag reduction system on the aerodynamics performance of the student formula car using numerical simulation." *AIP Conference Proceedings*. Vol. 2248. No. 1. AIP Publishing, 2020.
- [15] Dominy, R. G. "Aerodynamics of grand prix cars." *Proceedings of the Institution of Mechanical Engineers, Part D: Journal of Automobile Engineering* 206.4 (1992): 267-274.

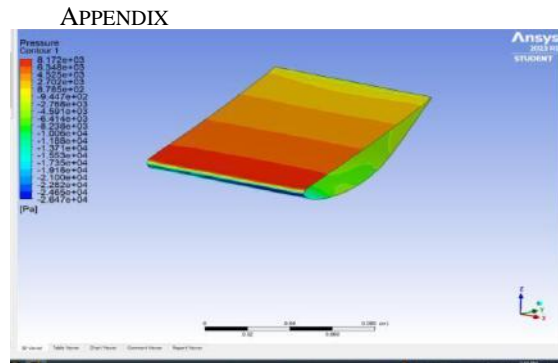


Fig 5. Pressure Contour of Single-wing

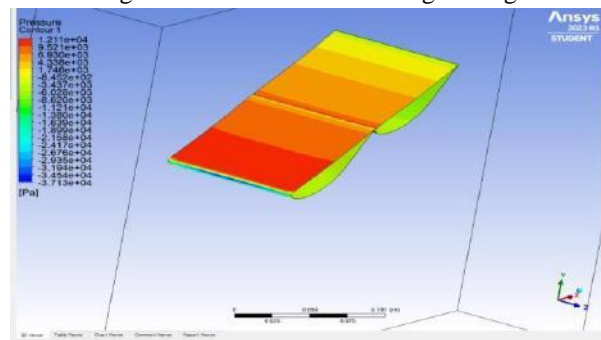
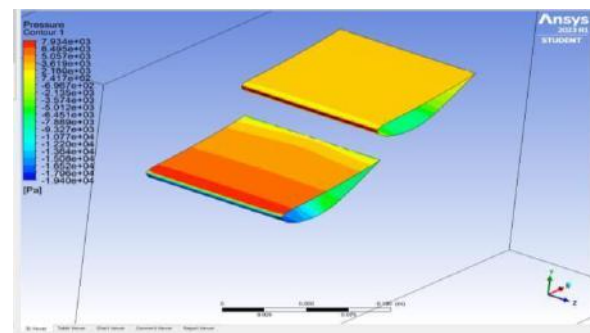


Fig 6. Pressure Contour of Double wing when DRS is



OFF.

Fig 7. Pressure Contour of Double wing when DRS is ON.